ACS APPLIED MATERIALS & INTERFACES

Research Article

www.acsami.org

Poly(ethylene oxide)−Poly(butylene oxide)−Poly(ethylene oxide)-Templated Synthesis of Mesoporous Alumina: Effect of Triblock Copolymer and Acid Concentration

Kelly L. Materna, Stacy M. Grant, and Mietek Jaroniec*

Department of Chemistry and Biochemistry, Kent State University, Kent, Ohio 44242, United States

ABSTRACT: Mesoporous alumina was synthesized via a one-pot self-assembly of aluminum isopropoxide and poly(ethylene oxide)-poly(butylene oxide)-poly(ethylene oxide) triblock copolymer in an acidic ethanol solution. The effects of the polymer concentration and nitric acid concentration, independently, on the adsorption properties (such as surface area, pore volume, microporosity, mesoporosity, and pore width) were studied. An increase in the specific surface area and the pore volume was seen for the samples containing a polymer/aluminum isopropoxide wt. ratio up to 0.71 and a polymer/acid wt ratio of 0.88. Titania isopropoxide was also added to the synthesis to illustrate the extension of this approach to alumina-based mixed metal oxides.

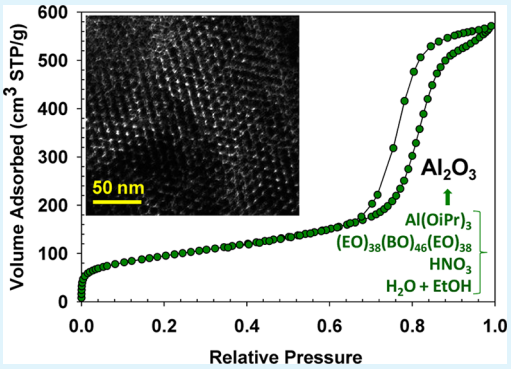

KEYWORDS: *mesoporous alumina, metal oxides, soft-templating, aluminum titanium oxide*

INTRODUCTION

Alumina is commonly used in a variety of applications such as catalysis,[1−4] optical[5] and biomedical[6] purposes, ceramics,[7,8] and adsorption.[9−11] The addition of supplementary metal oxides, such as titania (used extensively in catalysis and photocatalysis[12,13]), brings further applications to these materials. Titania-alumina materials can be used in automotives and aeronautics,[14] dental implants and orthopedics,[15] and the decontamination of chemical warfare agents.[16] Therefore, control of the properties such as surface area, pore width and porous structure of these materials, has attracted much attention. Mesoporous alumina (MA) has been synthesized through several routes, including the sol−gel method,[17,18] nonionic templating,[19] a reverse cation−anion double hydrolysis method (CADH),[20] and evaporation-induced self-assembly (EISA) with block copolymers.[21,22] Among various synthesis routes, the templating methods, especially those involving self-assembly, are particularly interesting because they allow for achieving high surface area of alumina samples and for tuning their porosity and surface properties.[2] A detailed comparison of different methods used for synthesis of templated mesoporous aluminas is presented in recent review,[2] which contains several tables listing experimental conditions and properties of these materials.

Niesz et al. reported a breakthrough in the block copolymer-templated synthesis of ordered mesoporous alumina (OMA) by showing the possibility of obtaining highly ordered alumina but at strict experimental conditions.[23] More recently, much attention has been directed toward block copolymer-templating synthesis because some of these polymers such as poly(ethylene oxide)-poly(propylene oxide)-poly(ethylene oxide) $[(EO)_n(PO)_m(EO)_n]$ known as Pluronics are inexpensive, biodegradable, commercially available and produce materials with large and uniform mesopores.[24] Another triblock copolymer, poly(ethylene oxide)-poly(butylene oxide)-poly(ethylene oxide), Vorasurf 504 $(EO)_{38}(BO)_{46}(EO)_{38}$, has been used in the synthesis of FDU-1 mesoporous silica producing siliceous materials with high surface areas (<714 cm^3/g)[25] and mesoporous alumina in a revised EISA synthesis, producing disordered materials with surface areas equal to 300 cm^3/g.[26]

In addition, adjustment of the acid concentration in a one-pot triblock copolymer-templated synthesis of mesoporous alumina permitted a good control of its structural parameters;[27] in this synthesis Pluronic P123 triblock copolymer $(EO)_{20}(PO)_{70}(EO)_{20}$ was used and the nitric acid concentration was varied to determine the effect acid concentration on the materials' adsorption characteristics. It was reported that the optimal range of nitric acid for the synthesis of mesoporous alumina with high surface areas (up to 467 m^2/g) and pore volume (0.74 cm^3/g) was 1.2−3.0 mols per one mol of aluminum isopropoxide;[27] this superior characteristics of mesoporous alumina stimulated us to study the acid concentration effect for another block copolymer template such as $(EO)_{38}(BO)_{46}(EO)_{38}$. This block copolymer has almost twice longer poly(ethylene oxide) blocks than those in Pluronic P123 but its middle block, poly(butylene oxide), is more hydrophobic than poly(propylene oxide) block in the

Received: May 15, 2012
Accepted: June 15, 2012
Published: June 15, 2012

   dx.doi.org/10.1021/am3008642 | ACS Appl. Mater. Interfaces 2012, 4, 3738−3744

aforementioned Pluronic, which favors the formation of body- and face-centered cubic mesostructures.

Furthermore, titania-alumina mesoporous materials have been previously synthesized using Pluronic P123 triblock copolymer, $(EO)_{20}(PO)_{70}(EO)_{20}$, varied quantities of titanium isopropoxide, and calcinations at increasing temperatures.[28] The resulting samples exhibited large surface areas (up to 438 m^2/g), pore uniformity, thermal stability up to 900 °C, and well-defined crystallinity.[28] The samples calcined at 900 °C with 5% to 10% titania did not show the presence of crystalline titania; as the percentage titania increases (20−75%), rutile, tielite, and anatase crystalline domains were present.[28] Lastly, the samples with less than or equal concentrations of titania to alumina showed ordering.[28]

Herein, we report the synthesis of mesoporous alumina and titania-alumina samples using Vorasurf 504 $(EO)_{38}(BO)_{46}(EO)_{38}$ triblock copolymer. These samples were prepared by using analogous recipes to those employed for the Pluronic P123-templated synthesis of ordered mesoporous alumina[21,29] and titania-alumina.[28] One-pot synthesis was used to obtain mesoporous alumina through the self-assembly of aluminum isopropoxide and $(EO)_{38}(BO)_{46}(EO)_{38}$ triblock copolymer. In addition, titanium isopropoxide was used in the synthesis of titania-alumina materials. The effect of the triblock copolymer and nitric acidic, independently, was studied.

EXPERIMENTAL SECTION

Synthesis of Mesoporous Alumina with Varied Polymer Concentration. Samples were prepared by mixing varied quantities of $(EO)_{38}(BO)_{46}(EO)_{38,}$ Vorasurf 504, with 20 mL of 99.5+% anhydrous ethanol (200 proof; Acros Organics) and stirring for four hours at room temperature. Sample MA-P1 contained 0.70 g of polymer; MA-P2, 0.95 g; MA-P3, 1.18 g; MA-P4, 1.45 g; MA-P5, 1.70 g; MA-P6, 1.94 g; where MA stands for mesoporous alumina and P represents polymer amount. Then, 2.0395 g of 98+% aluminum isopropoxide was added to the solution followed by 1.6 mL of 68 wt % HNO_3 and 20 mL of anhydrous ethanol. The final solution was stirred for five hours at room temperature and then placed in an oven for solvent evaporation at 60 °C for 48 h. The final samples were calcined at 400 °C in a horizontal quartz tube furnace in flowing air with a heating rate of 1 °C/min and held at 400 °C for 4 h. The molar composition of the synthesis mixture was as follows: AlP:P:HNO_3:EtOH = 9.99 × 10^{-3}:x:0.0261:0.343, where x = 1.02 × 10^{-4}, 1.38 × 10^{-4}, 1.72 × 10^{-4}, 2.11 × 10^{-4}, 2.47 × 10^{-4}, and 2.82 × 10^{-4} moles, and AlP denotes aluminum isopropoxide, P denotes the block copolymer, HNO_3 is nitric acid, and EtOH is ethanol. Furthermore, the six alumina samples, MA-P1 to MA-P6, were prepared with the following polymer/aluminum isopropoxide wt ratios: 0.34, 0.47, 0.58, 0.71, 0.83, and 0.95, respectively. The final samples were labeled as MA-Px, where MA stands for mesoporous alumina, P refers to the polymer concentration synthesis, and x is the sample number.

Synthesis of Mesoporous Alumina with Varied Nitric Acid Concentration. Eight samples were prepared by adding varied quantities of nitric acid to the synthesis mixtures used to obtain the MA-P3 and MA-P4 samples; the synthetic route was conducted in a manner identical to that of the polymer concentration synthesis. Samples MA-A1a and MA-A2a contained 0.98 mL of HNO_3; MA-A1b and MA-A2b, 1.30 mL; MA-A1c and MA-A2c, 1.60 mL; MA-A1d and MA-A2d, 1.95 mL, where A stands for the acid concentration synthesis. MA-A1a to MA-A1d contained 1.18 g of polymer, whereas MA-A2a to MA-A2d contained 1.45 g of polymer. Furthermore, the molar composition was as follows: AlP:P:HNO_3:EtOH = 9.99 × 10^{-3}:x:y:0.343, where x = 1.71 × 10^{-4} (MA-A1a to MA-A1d) or 2.11 × 10^{-4} moles (MA-A2a to MA-A2d) and y = 0.016 (MA-A1a and MA-A2a), 0.021 (MA-A1b and MA-A2b), 0.026 (MA-A1c and MA-A2c), and 0.032 mols (MA-A1d and MA-A2d). Lastly, the eight acid samples, MA-A1a to MA-A2d, were prepared with the following polymer to nitric acid weight ratio: 1.17, 0.88, 0.72, 0.59, 1.44, 1.09, 0.88, and 0.72, respectively. The final samples were labeled as MA-Azs where MA stands for mesoporous alumina; z is either 1 or 2, denoting the two different polymer concentrations used, and s changes from a through d, which stands for the volume of nitric acid added.

Synthesis of Mesoporous Alumina-Titania Samples. Alumina-titania samples were synthesized using a modified synthesis from a previously reported method.[30] Approximately 1.18 g of $(EO)_{38}$-$(BO)_{46}$-$(EO)_{38}$ triblock copolymer (Vorasurf 504) was dissolved in 20 mL of 99.5+% anhydrous ethanol (200 proof; Acros Organics) and stirred for four hours at room temperature. Then, 98+% aluminum isopropoxide, 1.6 mL of 68 wt % HNO_3, and 20 mL of anhydrous ethanol were added to the solution. Following, 98+% titanium(IV) isopropoxide (Acros Organics) was added dropwise to the solution. The final solution was stirred for five hours at room temperature and then placed in an oven for solvent evaporation at 60 °C for 48 h. Samples were then calcined in flowing air in a quartz tube furnace with a heating rate of 1 °C/min and held at 400, 700, or 900 °C for 4 h. The molar composition was as follows: AlP:P:HNO_3:EtOH:T = x:1.72 × 10^{-4}:0.0261:0.341:y, where T is the titanium isopropoxide molar value. For MA-10Ti-4, MA-10Ti-7, and MA-10Ti-9, x = 8.86 × 10^{-3} and y = 9.99 × 10^{-4}. Furthermore, for MA-20Ti-4, MA-20Ti-7, and MA-20Ti-9, x = 8.00 × 10^{-3}, and y = 2.00 × 10^{-3}. The final samples were labeled as MA-pTi-t where MA stands for mesoporous alumina, pTi stands for the percentage of titania in the sample, and t refers to the calcination temperature (in hundreds).

Measurements and Characterization. Nitrogen adsorption measurements were conducted using ASAP 2010 and ASAP 2020 (Micromeritics, Inc.) volumetric analyzers at −196 °C with ultra-high-purity nitrogen gas. Before measurement, all samples were outgassed under vacuum at 200 °C for 2 h.

Wide-angle and small-angle power X-ray diffraction (XRD) measurements were performed on an X'Pert Pro MPD multipurpose diffractometer (PANalytical, Inc.) with Cu Kα radiation (0.15406 nm) at room temperature. Wide angle measurements were conducted from 10 to 80° and small angle from 0.4° to 5.0°. A voltage of 40 kV, current setting of 40 mA, step size of 0.02°, and count time of 4s (wide angle) or 20s (small angle) were used for the measurements. The samples were placed on microscope glass slides for the analysis.

Transmission electron microscopy (TEM) images were obtained with an FEI Tecnai G2 F20 microscope. The accelerating voltage of the electron beam was 200 kV. The preparation of samples for TEM analysis involved sonication in ethanol for 2 to 5 min, deposition on a 600-mesh carbon coated copper grid and drying in a 60 °C oven.

Calculations. The BET surface area (S_{BET}) was calculated using the BET method in the relative pressure range of 0.05−0.2.[30] Nitrogen adsorption isotherm data were used to calculate the single-point pore volume (V_{sp}) at a relative pressure of 0.98. The volume of fine pores V_{mi} (mainly micropores) was calculated by integration of the pore size distribution (PSD) ujup to ~3 nm. The average pore width (w_{KJS}) was found at the maximum of the PSD curve.[30]

RESULTS AND DISCUSSION

Effect of Polymer Concentration on Mesoporous Alumina. Adsorption parameters such as the BET specific surface area, single-point pore volume, micropore volume and pore width, calculated from nitrogen adsorption data, are summarized in Table 1. As can be seen from this table, the BET specific surface area and pore volume increase with increasing polymer/aluminum isopropoxide wt. ratio up to 0.71. At higher polymer/aluminum isopropoxide ratios a significant drop is observed in these values. A small quantity of micropores (~0.01 cm^3/g) was observed for the samples containing a wt. ratio less than 0.83; however, a significant increase in microporosity (~0.07 cm^3/g) was observed for the samples with a wt. ratio of 0.83. Samples prepared by using ratios between 0.51 and 0.83 wt contain pore widths ranging from 10.4 to 13.7 nm.

Table 1. Adsorption Parameters of the Alumina Samples Prepared by Varying the Polymer/Alumina Precursor Ratio[a]

sample	P/a	S_{BET} (m^2/g)	V_{sp} (cm^3/g)	V_{mi} (cm^3/g)	w_{KJS} (nm)
MA-P1	0.34	329	0.42	0.02	8.0
MA-P2	0.47	364	0.78	0.01	10.9
MA-P3	0.58	343	0.87	0.00	10.4
MA-P4	0.71	451	0.91	0.01	10.8
MA-P5	0.83	400	0.54	0.07	13.7

[a] V_{sp} is the single point pore volume calculated from adsorption isotherm at $P/P_o = 0.98$; S_{BET} is the BET specific surface area obtained from the adsorption data in the P/P_o range from 0.05 to 0.2; V_{mi} is the micropore volume calculated by integration of PSD curve up to ~3 nm; w_{KJS} is the pore width calculated at the maximum of PSD; (P/a) is the polymer to aluminum isopropoxide wt ratio.

Panels a and b in Figure 1 display nitrogen adsorption isotherms and Figure 2 displays the PSD curves for the MA-P1

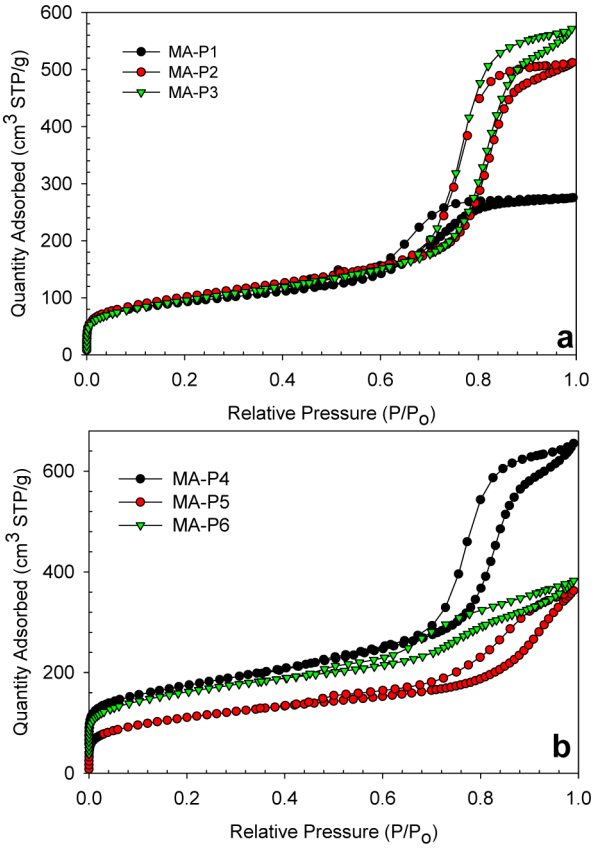

Figure 1. Nitrogen adsorption isotherms and pore size distribution curves for alumina samples prepared by varying polymer concentrations. (a) Isotherms for the samples from MA-P1 to MA-P3 and bottom panel; (b) isotherms for the samples from MA-P4 to MA-P6. The amount of polymer used increased in the order from P1 to P6 (see Table 1). The isotherm curves for MA-P4 and MA-P6 are shifted by 30 cm^3 STP/g.

to MA-P6 samples with polymer/aluminum isopropoxide ratio varying from 0.34 to 0.95. For all samples except MA-P1, MA-P5, and MA-P6 isotherms show a steep capillary condensation step, indicating a high uniformity of the mesopores. In comparison to MA-P1, MA-P5, and MA-P6, the capillary condensation step for the MA-P2 to MA-P4 samples shifts toward higher pressures, which suggests an increase in the pore

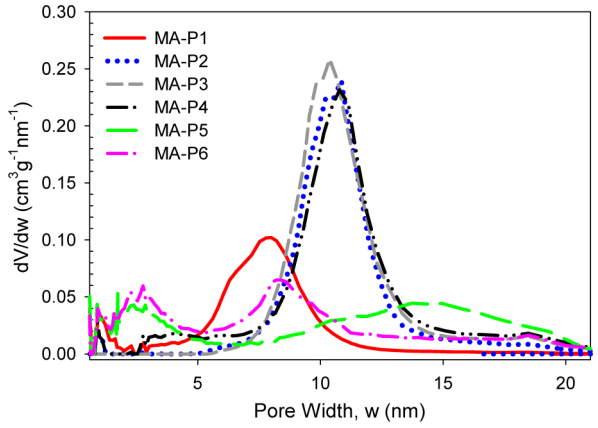

Figure 2. Pore size distribution curves for alumina samples shown in Figure 1.

width of the latter samples. In the case of MA-P3and MP-P4, this step is greater and steeper, indicating a larger volume of mesopores (see Table 1) and higher pore width uniformity. The smaller adsorption quantity and broader pore size distribution curves for MA-P5 and MA-P6 suggest a significant decrease in the pore volume and uniformity in these samples.

Furthermore, the pore size distributions for the MA-P2 to MA-P4 samples are narrow and centered at about 10−11 nm. The distribution curves for the samples with smallest and highest polymer/aluminum isopropoxide ratios studied are broader, smaller and shifted depending on the value of this ratio (see Figure 2).

Analysis of adsorption parameters and pore size distributions shows that the alumina samples with large pore volume were prepared within the specified range of the polymer/aluminum isopropoxide ratio, 0.47−0.71. In the aforementioned range, the pore width of 10−11 nm was achieved. The samples with much lower surface area and pore volume were obtained outside the aforementioned range, suggesting the suitable ratio of the block copolymer and aluminum isopropoxide should be maintained in order to obtain high surface area and large pore volume mesoporous alumina. It is also interesting to note a significant increase in microporosity in the case of the MA-P5 and MA-P6 samples. MA-P5 retains a large BET specific surface area and pore width, whereas MA-P6 retains a large pore width but its BET specific surface area is lower.

Figure 3 displays the small-angle X-ray diffraction patterns for the MA-P1 to MA-P6 samples. Structural ordering was observed through the well-defined peaks in Figure 3 for the samples prepared by using the polymer to alumina weight ratio from 0.47 to 0.71. Furthermore, the samples also had high BET specific surface area, pore width, and pore volume (Table 1). Confirmation of ordered mesoporosity in the samples is shown in Figure 4, which presents a TEM image for MA-P3. The wide-angle XRD patterns (not shown) are featureless, indicating amorphous nature of these samples, which is fully expected after calcination at 400 °C; similarly, the Pluronic P123-templated mesoporous alumina samples were also amorphous after calcination at 400 °C.[29]

Effect of Nitric Acid Concentration on Mesoporous Alumina. Samples MA-P3 and MA-P4 were further optimized by adjusting the acid concentration. Adsorption properties such as BET specific surface area, pore width, micropore volume, total pore volume, and pore width were analyzed for these samples; they are listed in Table 2. The samples labeled as "A1"

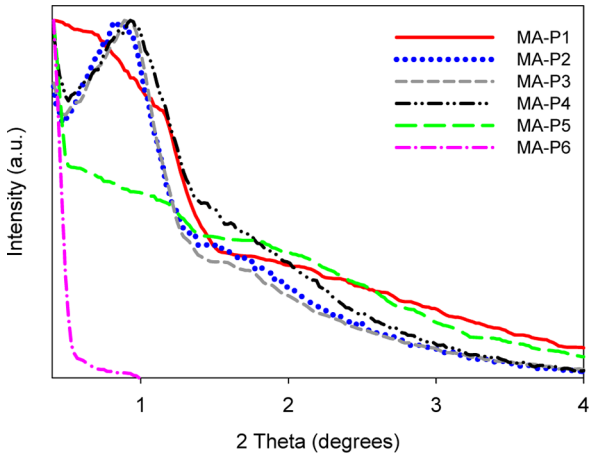

Figure 3. Small-angle XRD measurements for alumina samples shown in Figure 1.

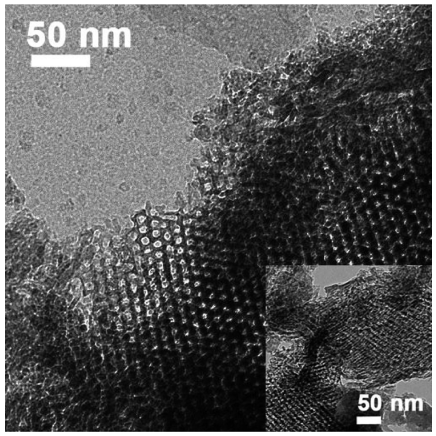

Figure 4. TEM images of the MA-P3 alumina sample prepared by using the polymer/alumina wt ratio = 0.58.

Table 2. Adsorption Parameters for Alumina Samples Prepared by Varying the Polymer/Acid Wt Ratio[b]

sample	P/N	S_{BET} (m^2/g)	V_{sp} (cm^3/g)	V_{mi} (cm^3/g)	w_{KJS} (nm)
MA-A1a	1.17	420	0.88	0.00	9.2
MA-A1b	0.88	397	0.93	0.00	10.1
MA-A1c	0.72	343	0.87	0.00	10.4
MA-A1d	0.59	407	0.66	0.04	11.2
MA-A2a	1.44	464	0.81	0.00	8.2
MA-A2b	1.09	437	0.90	0.00	9.6
MA-A2c	0.88	451	0.91	0.01	10.8
MA-A2d	0.72	427	0.66	0.04	11.1

[b] V_{sp} is the single point pore volume calculated from adsorption isotherm at P/P_o = 0.98; S_{BET} is the BET specific surface area obtained from the adsorption data in the P/P_o range from 0.05 to 0.2; V_{mi} is the micropore volume calculated by integration of PSD curve up to ~3 nm; w_{KJS} is the pore width calculated at the maximum of PSD; (P/N) is the polymer to nitric acid wt ratio.

were prepared using smaller amount of polymer and increasing acid concentration in the series from a to d. The surface area for the "A1" samples reaches a maximum of 420 m^2/g with a polymer to acid wt. ratio of 1.17. Moreover, the surface area of the "A1" samples decrease from 420 m^2/g to 343 m^2/g with polymer to nitric acid wt ratios of 1.17 to 0.72, but then increases again from 343 to 407 m^2/g with polymer to nitric acid wt ratios of 0.87 to 0.66. There is also a maximum pore volume at 0.93 cm^3/g with a polymer to nitric acid weight ratio of 0.88. The pore volume for these samples does not appear to increase or decrease specifically with acid concentration fluctuations. Instead, it stays in a range of 0.87−0.93 with polymer to nitric acid weight ratios of 0.72−1.17. However, there was a more significant decrease in pore volume to 0.66 cm^3/g with a polymer to nitric acid weight ratio of 0.59. Additionally, there is an increase in the pore width seen as nitric acid concentration increases, reaching a maximum of 11.2 nm with a polymer to nitric acid wt ratio of 0.59.

Furthermore, the samples labeled as "A2" used a higher concentration of polymer and were also labeled "a−d" as the nitric acid concentration increases in the samples. Unlike "A1" samples, the "A2" samples show a definite increase in the surface area as the acid concentration increases. In addition, the surface area reaches a maximum of 464 m^2/g and the pore volume to 0.91 cm^3/g at the polymer to acid wt. ratio of 1.44 and 0.88, respectively. The samples with high surface area and pore width (10.8−11.1 nm) were also obtained for the wt. ratio range from 0.72 to 0.88.

Figure 5a shows the adsorption isotherms for the MA-A1a to MA-A1d samples with polymer to acid wt. ratios of 0.59−1.17. Samples MA-A1a to MA-A1c show steep capillary condensation steps, indicating uniform pores. MA-A1d has a more broad capillary condensation step, demonstrating a decrease in uniformity in the sample. MA-A1b has the steepest and largest

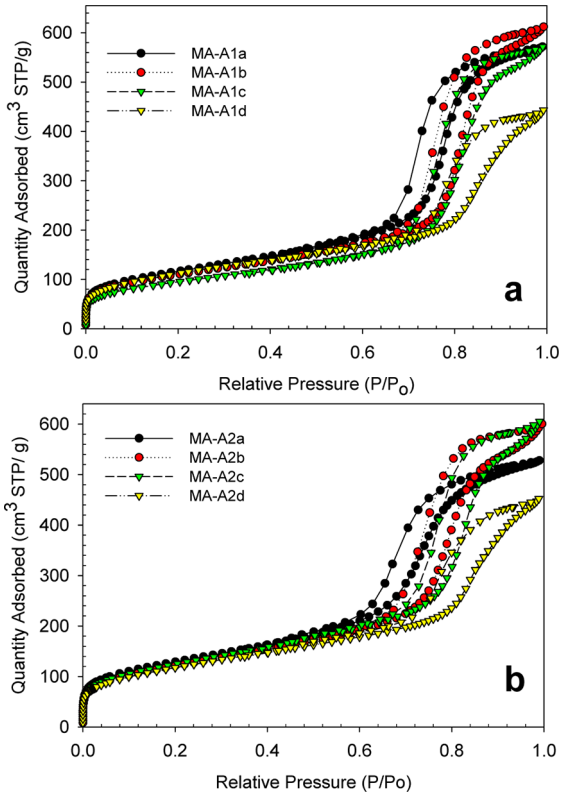

Figure 5. Nitrogen adsorption isotherms for alumina samples prepared by changing acid concentration. (a) MA-A1a to MA-A1d prepared using the polymer/alumina precursor ratio = 0.57, and (b) MA-A2a to MA-A2d obtained using the polymer/alumina precursor ratio = 0.71. However, the increasing acid concentration seen throughout the samples was kept consistent from a to d (see Table 2). For example, MA-A1a and MA-A2a contain the same amount of acid.

dx.doi.org/10.1021/am3008642 | ACS Appl. Mater. Interfaces 2012, 4, 3738−3744

capillary condensation step indicating large pore volume, pore width, and uniform porosity.

Figure 5b shows the adsorption isotherms for the MA-A2a to MA-A2d samples with a polymer to acid wt ratio of 0.72−1.44. All samples show steep capillary condensation steps indicating uniform pores. MA-A1c shows the steepest and largest capillary condensation step indicating a high pore width, uniform porosity, and large pore volume.

Furthermore, panels a and b in Figure 6 display the pore size distribution (PSD) curves for the aforementioned samples. In

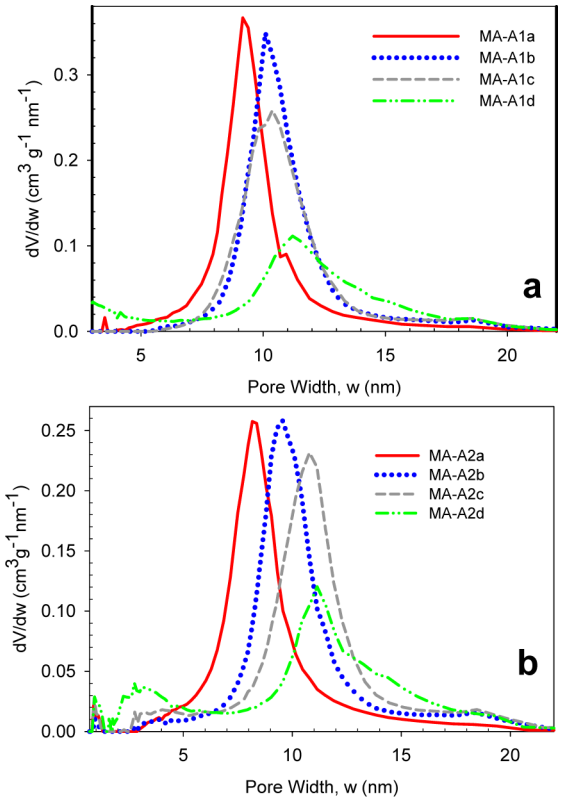

Figure 6. Pore size distribution curves for alumina samples studied correspond to the adsorption isotherms shown in panels a and b of Figure 5.

Figure 6a (MA-A1a to MA-A1d), MA-A1a and MA-A1b show narrow pore size distribution curves with pore widths ranging from 9.17 to 10.09 nm. The pore size distribution curves become broader from MA-A1c to MA-A1d, indicating an increase in the pore width and a decrease in the pore volume of these samples. MA-A1d is noteworthy because of its relatively high microporosity and large pore width (11.21 nm). Figure 6b (MA-A2a to MA-A2d) shows narrow pore size distribution curves for the MA-A2a to MA-A2c samples with pore widths in the range of (8.1−10.8 nm). The samples with higher pore width (around 11 nm) showed broader and smaller PSD curves indicating smaller volume of pores. Sample MA-A2d also stands out because of its high microporosity and large pore width (11.14), which is similar to the MA-A1d sample previously mentioned.

In addition, Figure 7 shows the small-angle X-ray diffraction patterns for "A1" samples. Structural ordering was observed due to well-defined peaks in the MA-A1a to MA-A1c samples with a polymer to acid wt. ratio range of 0.72−1.17. These samples also had high pore volume and surface area. The MA-A2a, MA-

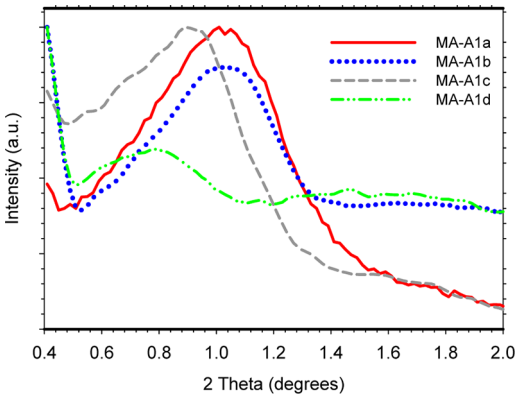

Figure 7. Small-angle XRD measurements for alumina samples MA-A1a-d.

A2b, and MA-A2d samples did not have any significant ordering present. These results suggest that altering acid concentration in the samples with a higher polymer concentration results in the samples without order, whereas the samples with a lower polymer concentration become more ordered as the acid concentration is adjusted up to 0.26 mol.

Recent studies on the role of acid in the polymer-templated synthesis of mesoporous silica[31,32] suggest that protons are involved in interactions between the PEO blocks and the silica precursors, which affect the micelle size. A similar effect can occur in the synthesis of mesoporous alumina. Because nitric acid acts as a catalyst for the hydrolysis of aluminum isopropoxide, and controls the reaction rate in metal alkoxide hydrolysis,[21] the acid concentration has a large effect on the mesostructure formation. Furthermore, the pore width generally increases as acid concentration increases, which could be a result of the increase in H^+ and NO_3^- ions in solution, creating a saltlike effect.[27] The increased amount of water that is associated with 68$^+$% nitric acid could also cause swelling of the hydrophilic core, resulting in the larger pore width.[27] Moreover, the samples labeled as "A1" show a similar trend in adsorption properties such as higher adsorption at lower acid concentration as compared to the samples previously synthesized with Pluronic P123 triblock copolymer $(EO)_{20}(PO)_{70}(EO)_{20}$.[27] Both samples also showed an increase in the pore width as the acid concentration increases, which could be from the saltlike effect of the H^+ and NO_3^- ions in solution.[27]

Addition of Titania to Mesoporous Alumina. Adsorption characteristics of titania-alumina samples can be found in Table 3. Panels a and b in Figure 8 show adsorption isotherms and pore size distribution curves for the titania-alumina samples. The samples calcined at 400 °C with 10 and 20% titania were observed to have larger surface area and pore volume than the samples calcined at higher temperatures. However, the samples calcined at 900 °C showed a significant increase in the pore width, ranging from 17 to 18 nm, which has been observed in previously reported titania-alumina samples.[28] Also, the samples calcined at higher temperature (900 °C) exhibit steeper capillary condensation steps indicating pore size uniformity. Those calcined at 400 and 700 °C also have steep capillary condensation steps but they are slightly broader in the case of the samples calcined at 900 °C, which could be due to the well-defined crystallinity present in the latter samples.

dx.doi.org/10.1021/am3008642 | ACS Appl. Mater. Interfaces 2012, 4, 3738−3744

Table 3. Adsorption Properties of Titanium Aluminum Oxide Samples Studied[c]

sample	S_{BET} (m^2/g)	V_{sp} (cm^3/g)	V_m (cm^3/g)	w_{KJS} (nm)
MA-10Ti-4	277	0.44	0.02	10.4
MA-10Ti-7	177	0.36	0.01	10.1
MA-10Ti-9	68	0.27	0.00	17.5
MA-20Ti-4	299	0.48	0.03	10.8
MA-20Ti-7	199	0.44	0.00	10.8
MA-20Ti-9	60	0.26	0.00	18.8

[c] V_{sp} is the single point pore volume calculated from adsorption isotherm at $P/P_o = 0.98$; S_{BET} is the BET specific surface area obtained from the adsorption data in the P/P_o range from 0.05 to 0.2; V_{mi} is the micropore volume calculated by integration of PSD curve up to ~3 nm; w_{KJS} is the pore width calculated at the maximum of PSD.

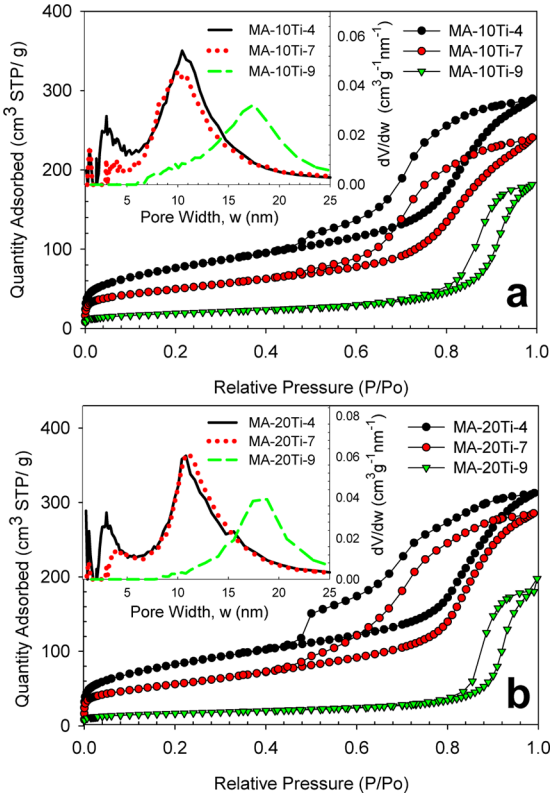

Figure 8. Nitrogen adsorption isotherms and pore size distribution curves (insets) for the titania-alumia samples studied.

Wide-angle XRD, Figure 9, was obtained for the samples calcined at 900 °C, which show crystallinity as characterized by the sharp peaks in the XRD patterns. Samples at 400 °C are amorphous and begin showing crystallinity at 700 °C, which has been previously reported[28] in similar materials. The sample with 10% titania shows peaks identifying the material as aluminum oxide (al), whereas the sample with 20% titania shows peaks for both anatase (a) and aluminum oxide. At lower molar fractions of titania (10%) there may be insufficient titanium in the sample to resolve individual peaks for titanium oxide (TiO_2) or a mixed phase titanium–aluminum oxide. At 20% titanium one can expect that there would be alumina present due to the molar excess and either titanium oxide or tielite (Al_2TiO_5). Because of the fact that there is anatase present in this sample, it is likely that the titanium is present as an individual phase which differs from previous studies of mesoporous titania-alumina oxide.[28]

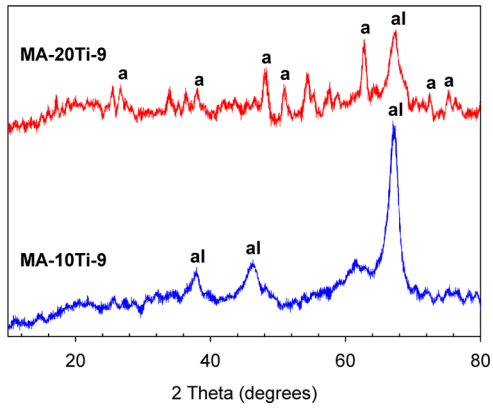

Figure 9. Wide-angle X-ray diffraction patterns for 10 and 20% titania-alumina samples calcined at 900 °C. XRD patterns were assigned as follows: MA-10Ti-9 (JCPDS 4–874, η-alumina) and MA-20Ti-9 (JCPDS 4–875, η-alumina and JCPDS 21–1272, anatase). Peaks were labeled "a" for anatase and "al" for aluminum oxide.

CONCLUSIONS

Mesoporous alumina samples with high surface area and large pore volume were successfully synthesized in the presence of the triblock copolymer $(EO)_{38}(BO)_{46}(EO)_{38}$ using aluminum isopropoxide in nitric acid–acidified ethanol. The samples prepared by varying the polymer concentration and thus, the polymer/aluminum isopropoxide weight ratio, up to 0.71, showed large pore volume and high BET specific surface area. An analogous behavior was observed for the samples prepared by changing the acid concentration. The alumina samples with high BET specific surface area and large pore volume have the potential to be used in various adsorption and catalysis applications. The addition of titania to the synthesis provided samples with high pore width and surface area.

AUTHOR INFORMATION

Corresponding Author

*Phone: 330-672-3790. Fax: 330-672-3816. E-mail: jaroniec@kent.edu.

Notes

The authors declare no competing financial interest.

ACKNOWLEDGMENTS

The TEM data were obtained at the (cryo) TEM facility at the Liquid Crystal Institute, Kent State University, supported by the Ohio Research Scholars Program *Research Cluster on Surfaces in Advanced Materials*. The authors thank Dr. Min Gao for technical support with the TEM experiments and the Dow Chemical Co. for providing the Vorasurf 504 triblock copolymer used in this study. This work was partially supported by the National Science Foundation under CHE-0649017 (REU) grant; M.K., undergraduate student from Kent State University (KSU), participated in the REU 2011 summer program at KSU.

REFERENCES

(1) Khaleel, A.; Shehadi, I.; Al-Marzouqiu, A. *Fuel Process. Technol.* **2011**, *92*, 1783.
(2) Marquez-Alvarez, C.; Zilkova, N.; Perez-Pariente, J.; Čejka, J. *Catal. Rev.* **2008**, *50*, 222.
(3) Khaleel, A. *Microporous Mesoporous Mater.* **2006**, *91*, 53.
(4) Seki, T.; Onaka, M. *Catalyis Surveys Asia.* **2006**, *10*, 138.

(5) Chandra, A.; Turng, L. S.; Gopalan, P.; Rowell, R. M.; Gong, S. *J. Appl. Polym. Sci.* **2007**, *105*, 2728.
(6) Kim, Y.; Anirban, J.; Song, H. *J. Biomater. Appl.* **2011**, *25*, 539.
(7) Badmos, A.; Ivey, D. *J. Mater. Sci.* **2001**, *36*, 4495.
(8) Park, J.; You, S.; Shin, D.; Ozturk, A. *Mater. Chem. Phys.* **2010**, *124*, 113.
(9) Yu, M.; Li, X.; Ahn, W. *Microporous Mesoporous Mater.* **2008**, *113*, 197.
(10) Jagtap, S.; Yenkie, M.; Labhsetwar, N.; Rayalu, S. *Microporous Mesoporous Mater.* **2011**, *142*, 454.
(11) Chen, C.; Ahn, W. *Chem. Eng. J.* **2011**, *166*, 646.
(12) Mishra, H.; Stancciulescu, J.; Charland, P.; Kelly, J. *Appl. Surf. Sci.* **2008**, *254*, 7098.
(13) Ma, Q.; Quin, T.; Liu, S.; Weng, L.; Dong, W. *Appl. Phys. A: Mater. Sci. Process.* **2011**, *104*, 365.
(14) Mas-Guindal, M.; Benko, E.; Rodriguez, J. *J. Alloys Compd.* **2008**, *454*, 352.
(15) Kim, S.; Lim, J.; Lee, S.; Nam, C.; Kang, G.; Choi, J. *Electrochim. Acta* **2008**, *53*, 4846.
(16) Wagner, C.; Procell, L.; Munavalli, S. *J. Phys. Chem.* **2007**, *111*, 17564.
(17) Saha, S. *J. Sol−Gel Sci. Technol.* **1994**, *3*, 117.
(18) Le Bihan, L.; Dumeignil, F.; Payen, E.; Grimblot, J. *J. Sol−Gel Sci. Technol.* **2002**, *24*, 113.
(19) Deng, W.; Bodart, P.; Shanks, B. *Microporous Mesoporous Mater.* **2002**, *52*, 169.
(20) Bai, P.; Wu, P.; Yan, Z.; Zhao, X. *Microporous Mesoporous Mater.* **2009**, *118*, 288.
(21) Yuan, Q.; Yin, A.; Luo, C.; Sun, L.; Zhang, Y.; Duan, W.; Liu, H.; Yan, C. *J. Am. Chem. Soc.* **2008**, *130*, 3465.
(22) Kuemmel, M.; Grosso, D.; Boissiere, C.; SMarsly, B.; Brezesinski, T.; Albouy, P.; Amenitsch, H.; Sanchez, C. *Angew. Chem., Int. Ed.* **2005**, *44*, 4589.
(23) Niesz, K.; Yang, P; Somorjai, G. A. *Chem. Commun.* **2005**, *15*, 1986.
(24) Yang, P.; Zhao, D.; Margolese, D.; Chmelka, B.; Stucky, G. *Nature* **1998**, *396*, 152.
(25) Cides da Silva, L.; dos Reis, T.; Cosentino, I.; Fantini, M.; Matos, J.; Bruns, R. *Microporous Mesoporous Mater.* **2010**, *133*, 1.
(26) Cai, W.; Yu, J.; Jaroniec, M. *J. Mater. Chem.* **2011**, *21*, 9066.
(27) Grant, S.; Jaroniec, M. *J. Mater. Chem.* **2011**, *21*, 86.
(28) Morris, S.; Horton, J.; Jaroniec, M. *Microporous Mesoporous Mater.* **2010**, *128*, 180.
(29) Morris, S.; Fulvio, P.; Jaroniec, M. *J. Am. Chem. Soc.* **2008**, *130*, 15210.
(30) Kruk, M.; Jaroniec, M. *Chem. Mater.* **2001**, *13*, 3169.
(31) Baute, D.; Goldfarb, D. *J. Phys. Chem. C.* **2007**, *111*, 10931.
(32) Caragheorgheopol, A.; Rogozea, A.; Ganea, R.; Florent, M.; Goldfarb, D. *J. Phys. Chem. C* **2010**, *114*, 28.